

Compact Acid-Induced State of *Clitoria ternatea* Agglutinin Retains Its Biological Activity

A. Naeem^{1,2}, M. Saleemuddin^{1,2}, and R. H. Khan^{1*}

¹Interdisciplinary Biotechnology Unit, Aligarh Muslim University, Aligarh 202002, India; fax: +91-571-2721776; E-mail: rizwanhkh@hotmai.com

²Department of Biochemistry, Life Science, AMU, Aligarh 202002, India

Received January 5, 2009

Revision received March 25, 2009

Abstract—The effects of pH on *Clitoria ternatea* agglutinin (CTA) were studied by spectroscopy, size-exclusion chromatography, and by measuring carbohydrate specificity. At pH 2.6, CTA lacks well-defined tertiary structure, as seen by fluorescence and near-UV CD spectra. Far-UV CD spectra show retention of 50% native-like secondary structure. The mean residue ellipticity at 217 nm plotted against pH showed a transition around pH 4.0 with loss of secondary structure leading to the formation of an acid-unfolded state. This state is relatively less denatured than the state induced by 6 M guanidine hydrochloride. With a further decrease in pH, this unfolded state regains ~75% secondary structure at pH 1.2, leading to the formation of the A-state with native-like near-UV CD spectral features. Enhanced 8-anilino-1-naphthalene-sulfonate binding was observed in A-state, indicating a “molten-globule” like conformation with exposed hydrophobic residues. Acrylamide quenching data exhibit reduced accessibility of quencher to tryptophan, suggesting a compact conformation at low pH. Size-exclusion chromatography shows the presence of a compact intermediate with hydrodynamic size corresponding to a monomer. Thermal denaturation of the native state was cooperative single-step transition and of the A-state was non-cooperative two-step transition. A-State regains 72% of the carbohydrate-binding activity.

DOI: 10.1134/S0006297909100046

Key words: acid-induced unfolding, *Clitoria ternatea* agglutinin, carbohydrate binding, molten-globule state, thermal stability

To understand factors governing the formation of three-dimensional protein structures, it is important to elucidate the hierarchy of interactions that stabilize the native and molten-globule states. A molten globule exists as an intermediate between native and denatured states. It is defined as a compact conformation with a comparable amount of native-like secondary structure but with a large enhancement in the intramolecular motion, i.e. largely disordered tertiary structure [1-3]. There are evidences that support the idea that the molten globule might also possess well-defined tertiary contacts [4-6].

The high cooperativity and complexity of the protein folding process makes the characterization of conforma-

tional transitions and equilibrium intermediate states extremely difficult [7, 8]. One of the main challenges of the “protein folding problem” is the characterization of the partially folded stable intermediate states [9]. Several studies have shown that the amount of secondary structure and the compactness of the intermediate state formed in the folding pathway of a protein are not necessarily close to those of the native state, but vary greatly [10, 11]. This suggests the formation of various intermediate states, from one close to the fully unfolded state to that close to the native protein [8, 9, 11-13]. Characterization of such intermediate states is an important task in protein folding studies [10, 14, 15].

Lectins are proteins or glycoproteins of non-immune origin that agglutinate cells and precipitate complex carbohydrates and polysaccharides. *Clitoria ternatea* agglutinin (CTA) is a dimeric galactose-specific novel lectin obtained from *C. ternatea* seeds. A number of conformational studies have been reported with different lectins. The conformational studies regarding this novel lectin are

Abbreviations: ANS, 8-anilino-1-naphthalene-sulfonic acid; A-state, acid induced state; CTA, *Clitoria ternatea* agglutinin; GdnHCl, guanidine hydrochloride; MRE, mean residue ellipticity; SEC, size-exclusion chromatography; UA, acid unfolded state.

* To whom correspondence should be addressed.

yet to be investigated. In this present communication, we report the presence of a partially folded intermediate termed "acid unfolded" (UA) and a molten globule termed "A-state". The former have disordered side chains with loss of secondary structure hence loss of activity. The latter have native-like secondary as well as tertiary structure with a regain in the activity.

MATERIALS AND METHODS

CTA was purified from the seeds of *C. ternatea* [16, 17]. Homogeneity was checked by SDS-PAGE [18]. All chemicals used in this study were of analytical grade.

All the measurements were carried out at room temperature. Typically, protein stock solution (5 mg/ml) was prepared in and dialyzed against 20 mM sodium phosphate buffer, pH 7.0. In pH studies, the following 20 mM buffers were used: glycine-HCl (pH 0.8-2.2), sodium acetate (pH 2.5-6.0), and sodium phosphate (pH 7.0). After adding the appropriate buffer to the stock protein solution, the samples were incubated at room temperature for 3 h prior to spectroscopic measurements. The concentration of native protein was determined by the procedure described by Lowry et al. [19].

Fluorescence measurements. Fluorescence spectra were recorded with a Shimadzu RF 540 spectrofluorimeter (Japan) in a 10 mm pathlength quartz cell. The excitation wavelength was 280 nm and the emission was recorded from 300 to 500 nm. The final protein concentration was 15 μ M for all fluorescence measurements [20].

Circular dichroism (CD) measurements. CD was measured with a Jasco J 720 spectropolarimeter calibrated with ammonium d-10 camphor sulfonate. A cell of pathlength 0.1 or 1 cm was used for scanning between 250-190 and 300-250 nm, respectively. Each spectrum was the average of four scans. Protein concentrations of the samples were typically 20 μ M for far-UV CD and 50 μ M for near-UV CD studies. The results were expressed as the mean residue ellipticity (MRE in $\text{deg}\cdot\text{cm}^2\cdot\text{dmol}^{-1}$), which is defined as $\text{MRE} = \theta_{\text{obs}} (\text{mdeg}) / (10n C_p l)$, where θ_{obs} is the observed ellipticity in degrees, n is the number of amino acid residues in the protein, C_p is the molar fraction, and l is the length of light path in cm.

ANS-fluorescence measurements. ANS (8-anilino-1-naphthalene-sulfonate) binding was measured by fluorescence emission with excitation at 380 nm and emission was recorded from 400 to 600 nm. Typically, ANS concentration was 100-fold molar excess of protein concentration and protein concentration was in the vicinity of 15 μ M [21-24].

Acrylamide quenching. Aliquots of 5 M acrylamide stock solution were added to a protein stock solution (15 μ M) to achieve the desired acrylamide concentration.

Excitation was set at 295 nm in order to excite tryptophan only, and the emission spectrum was recorded in the range 300-400 nm. The slit width was set at 10 nm for both excitation and emission. The data were interpreted according to Stern-Volmer and modified Stern-Volmer plots. The decrease in fluorescence intensity at λ_{max} was analyzed according to the Stern-Volmer equation:

$$F_0/F = 1 + K_{\text{SV}}[Q],$$

where F_0 and F are the fluorescence intensities at an appropriate wavelength in the absence and presence of a quencher (acrylamide), respectively; K_{SV} is the Stern-Volmer constant, and $[Q]$ is the concentration of the quencher [25].

Size-exclusion chromatography (SEC). SEC experiments were performed on a Sephadex G-200 (76 \times 1.15 cm) column. The column was pre-equilibrated with 20 mM sodium phosphate buffer, pH 7.0, or 20 mM glycine-HCl for pH 2.6 and 1.2. Two milliliters of 3 mg/ml native lectin and lectin preincubated at pH 2.6 or 1.2 were applied to the column and eluted at 20 ml/h. The eluted fractions were read at 280 nm. The molecular mass markers used were glucose oxidase (160 kDa), Con A (104 kDa), BSA (66.7 kDa), ovalbumin (45 kDa), lactoglobulin (33 kDa), chymotrypsinogen (25.5 kDa), soybean trypsin inhibitor (20 kDa), lysozyme (14 kDa), and cytochrome *c* (12.5 kDa).

Oligomeric structure. The oligomeric status of acid-induced unfolding intermediates of CTA was determined under non-denaturing conditions by the method of Davis [18]. Proteins were visualized by staining with Coomassie brilliant blue R-250.

Thermal studies. To determine the thermal stability of the intermediate state relative to native, MRE changes at 217 nm and relative fluorescence were measured as a function of temperature. Temperature was continuously varied from 25 to 85°C at a constant rate by carefully adjusting the heating control of the water bath. Measurements were made after 5 min to allow for thermal equilibrium at the desired temperature, and f_D (fraction of protein denatured) was calculated.

Precipitation reaction. The interaction of CTA (0.5 mg/ml) with mucin (1.5 mg/ml) was studied in 10 mM Tris-HCl buffer, pH 7.0, containing metal ions (Ca^{2+} , Mn^{2+}) by a turbidity method at 350 nm on a Hitachi model U 1500 spectrophotometer (Hitachi, Japan) and was plotted in terms of percentage [12]. For each sample, proper blanks of lectin and polysaccharide were taken into account.

RESULTS

The unfolding of *C. ternatea* agglutinin was studied over the pH range 0.8-7.0. To detect and characterize the

protein structure, measurements of near-UV CD, intrinsic tryptophan fluorescence, and ANS binding were used. Far-UV CD was used to quantify secondary structure, and size-exclusion chromatography was employed for hydrodynamic studies.

Intrinsic fluorescence. The intrinsic fluorescence of the fluorophore tryptophan is an excellent parameter to monitor the polarity of the tryptophan environment in the protein and is highly sensitive to the environment [20]. The modification of microenvironment of tryptophan residues has been monitored by studying the changes in the intensity and wavelength of emission of tryptophan fluorescence as the function of pH (Fig. 1). CTA contains four tryptophan and six tyrosine residues in each subunit [17]. With progressive decrease in pH down to 2.6, the relative fluorescence intensity gradually decreases, indicating that the lectin conformation is being altered. A clear transition can be seen in Fig. 1a, where around pH 4.0 the lectin undergoes a sharp decrease in fluorescence intensity as well as emission maxima (inset), which stabilizes at pH 2.6. Figure 1a inset shows that the emission maximum (λ_{\max}) is blue shifted by approximately 7 nm as the lectin encounters low pH, which indicates that the microenvironment of aromatic amino acids is becoming less polar. Beyond this pH, however, the fluorescence intensity of tryptophan is found to increase with an accompanying red shift in λ_{\max} , suggesting the tryptophan residues are again relocating into a relatively more polar region.

The emission spectra of CTA at pH 7.0 (Fig. 1b, curve 2) show a maximum at 342 nm, which suggests that some tryptophan residues are buried and others are relatively more exposed to the solvent. At pH 2.6, the fluorescence intensity is quenched with an accompanying decrease in emission maximum (curve 4). This blue shift of 7 nm can be attributed to conformational changes in the vicinity of

the surface exposed tryptophan causing their internalization. A similar blue shift has been reported for glucose isomerase [26], bovine growth hormone [27], and interferon- γ [28]. The addition of 2 M urea to the lectin at pH 2.6 further decreases the fluorescence intensity, apparently without altering the microenvironment of the aromatic fluorophore (curve 5). At pH 1.2, there is an increase in fluorescence intensity with increase in λ_{\max} (curve 3). The denatured protein (6 M guanidine hydrochloride (GdnHCl) at pH 7.0) gives rise to an emission maximum at 352 nm (the normal emission maximum for tryptophan in solution), a red shift of ~ 10 nm with a concomitant increase in the fluorescence intensity, suggesting the presence of a completely unfolded state with all the tryptophans exposed to the environment (curve 1). This indicates that the lectin at low pH exists in a conformational state that is different from the native as well as the completely unfolded state in the presence of 6 M GdnHCl.

CD measurements. The changes in the secondary structure of CTA as a function of pH were followed by far-UV CD by measuring mean residue ellipticity values at 217 nm (Fig. 2a). A cooperative transition from native to unfolded state (pH 2.6) occurs near pH 4.0, reflecting the loss of secondary structure. The protonation of carboxyl groups leads to sufficient net positive charge in the CTA to trigger the electrostatically driven unfolding transition. Further addition of HCl down to pH 1.2 leads to a second transition manifested as a regain of a significant amount of lost secondary structure due to the effective shielding of repulsive forces by the anions leading to the A-state, with properties of a molten globule, e.g. an amount of secondary structure comparable to that in the native state. Acid titration in the presence of 50 mM KCl can lead directly from the native to the A-state without the intermediacy of the UA (acid unfolded) state. The presence of KCl resulted

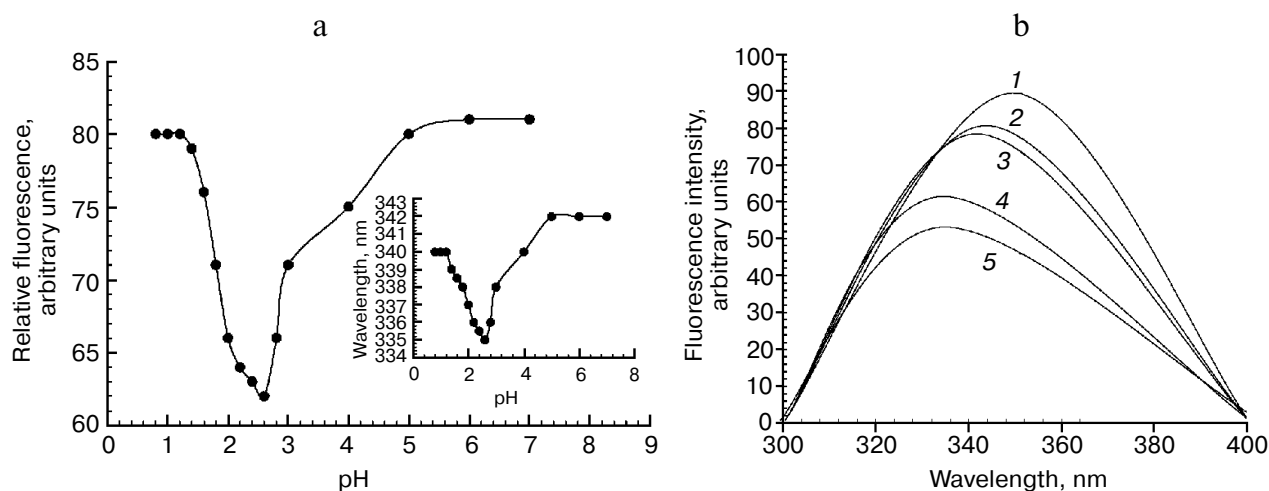


Fig. 1. Effect of pH on the fluorescence emission intensity of CTA excited at 280 nm at 25°C. a) Relative fluorescence intensity as a function of pH; inset, emission wavelength maximum versus pH. b) Fluorescence emission spectra of CTA: 1) pH 7.0 + 6 M GdnHCl; 2) native CTA; 3) pH 1.2; 4) pH 2.6; 5) pH 2.6 + 2 M urea. The protein concentration was 15 μ M and the pathlength was 0.1 cm.

in a shift in the position of the transition from the native to denatured state to somewhat higher pH values. Figure 2b shows the far-UV CD spectrum of CTA for the native state with the minimum at 217 nm (curve 4). The difference between the CD spectrum of the UA state (pH 2.6) (curve 2) and that in the presence of 6 M GdnHCl (curve 1) reflects the presence of some secondary structure. At pH 2.6, CTA shows a maximal loss of 50% β sheet structure (curve 2). However, at pH 1.2, CTA shows spectral features close to those of native lectin with 75% β -sheet content (curve 3). The CD spectrum in the near-UV region was used to probe the asymmetry of the aromatic amino acid environment of the protein (Fig. 2c). The near-UV CD spectrum of native CTA shows a prominent positive band at 275 nm (curve 1). The loss of tertiary structure at pH 2.6 can be seen by decrease in band intensity (curve 3). In the aromatic region, a loss of CD signal reflects the loss of the native-like tertiary structure. This loss of secondary as well as tertiary structure yields the acid-unfolded state, UA. Almost 66% of the tertiary structure is lost. CTA at pH 2.6 still retains some tertiary structure (~34%) as observed by a greater decrease in band intensity in the presence of 6 M GdnHCl (curve 4). However, CTA regains a significant amount of tertiary structure at pH 1.2 (A-state), close to the native state (curve 2).

ANS binding. Binding of ANS to the hydrophobic regions of proteins results in an increase in fluorescence intensity, which has been widely used to detect the molten globule states of various proteins [22–24]. This property of ANS was also used to study the pH-induced unfolding of CTA (Fig. 3). ANS shows minimal binding in the pH range 3.0–7.0. ANS fluorescence shows a gradual increase at pH 2.6 and reaches a maximum at pH 1.2. At still lower pH, ANS fluorescence is decreased, suggesting reorganization of the lectin conformation leading to burial of hydrophobic regions in the CTA interior (Fig. 3a). At pH 1.2, the ANS fluorescence emission of CTA decreases relative to native from 510 to 480 nm, i.e. from free ANS in water to protein-bound ANS. A blue shift of approximately 35 nm was observed (inset). Comparative ANS fluorescence emission spectra in the 400–600 nm range are shown in Fig. 3b. Native CTA showed negligible ANS binding (curve 4). At pH 2.6, an increase in fluorescence emission is observed, indicating the presence of residual structure in the UA state to which ANS binds (curve 3). At pH 1.2, a very substantial emission signal is observed, reflecting the preferential binding of ANS to the A-state (curve 2). However, in the presence of 50 mM KCl at pH 2.6, CTA showed enhanced ANS binding overlapping the spectrum of the A-state (curve 1). Thus, it appears that the acid-induced state, although retaining a significant amount of native-like secondary and tertiary structures, also has sizeable amounts of exposed hydrophobic regions. This suggests the accumulation of a compact “molten globule”-like intermediate at low pH possessing persistent tertiary as well as secondary structure.

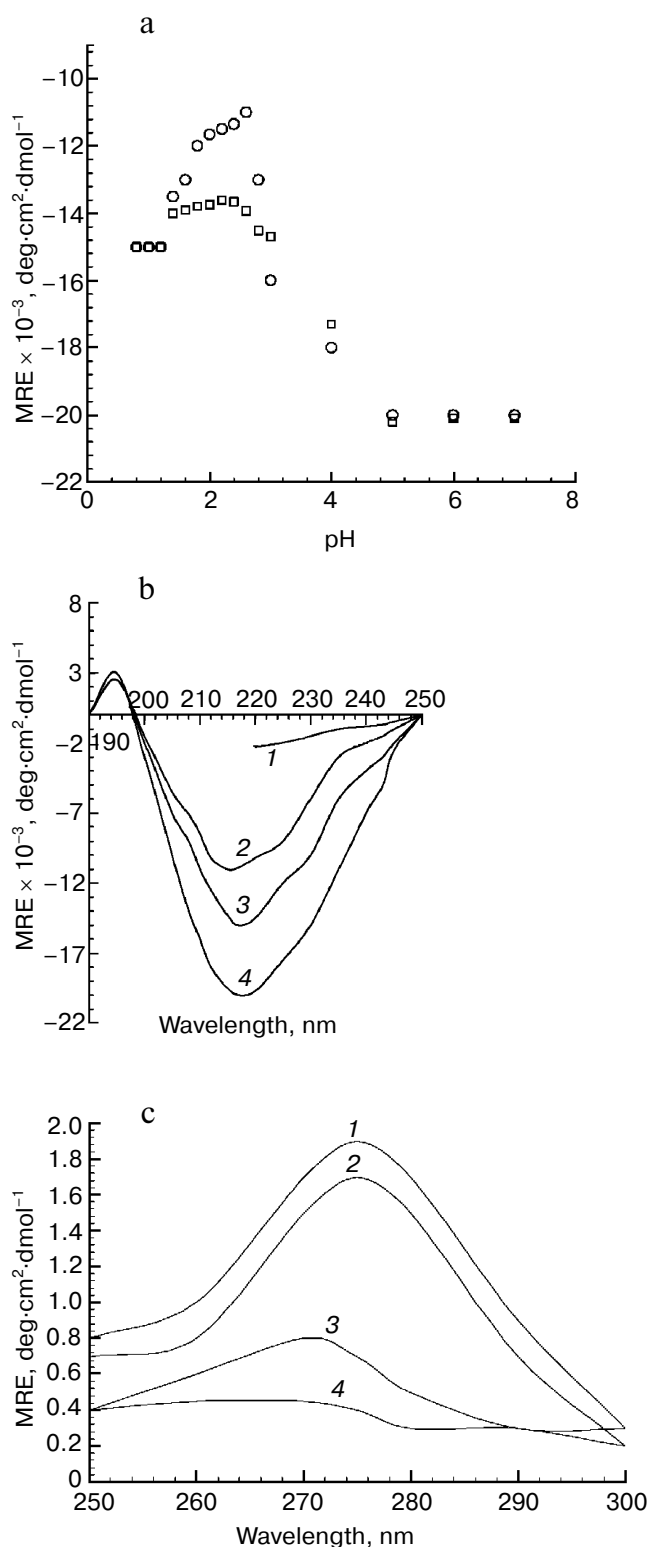


Fig. 2. CD spectra of CTA as a function of pH at 25°C. a) MRE was measured at 217 nm as a function of pH by far-UV CD. b) Spectra of CTA: 1) pH 7.0 + 6 M GdnHCl; 2) pH 2.6; 3) pH 1.2; 4) native CTA. The protein concentration was 15 μ M and the pathlength was 0.1 cm. c) Near-UV CD: 1) native CTA; 2) pH 1.2; 3) pH 2.6; 4) pH 7.0 + 6 M GdnHCl. The protein concentration was 30 μ M and the pathlength was 1 cm.

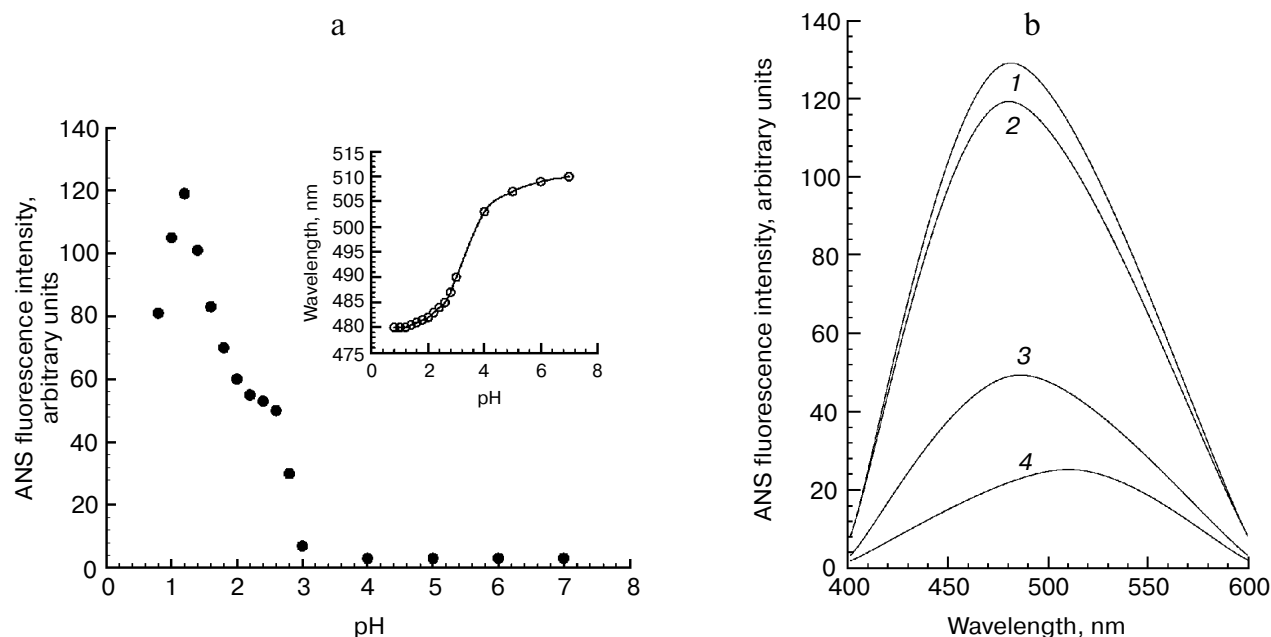


Fig. 3. Fluorescence of ANS binding to CTA as a function of pH (excited at 380 nm at 25°C). a) ANS fluorescence intensity versus pH; inset, wavelength emission maxima versus pH. b) ANS fluorescence emission spectra: 1) pH 2.6 + 50 mM KCl; 2) at pH 1.2; 3) at pH 2.6; 4) native CTA.

Acrylamide quenching. The fluorescence properties of Trp residues can be used to obtain topological information on proteins. Fluorescence quenching of the tryptophanyl residues by different quenchers has been shown to be useful to obtain information about the solvent accessibility of these residues in proteins and the polarity of their

microenvironment [25, 29]. However, quenchers like acrylamide can penetrate into a protein and give rise to normal Stern–Volmer kinetics. The increase in slope of the Stern–Volmer plot indicates ready accessibility of tryptophan residues to the quencher. Figure 4 depicts the Stern–Volmer and modified Stern–Volmer plots (inset) for the acrylamide quenching studies performed on the three states of CTA. The results indicate that the degree of quenching of CTA increases as the pH is lowered, which indicates greater exposure of tryptophans. This implies that tryptophans are maximally exposed at pH 7.0, relatively less exposed to quencher at pH 1.2, and least accessible to quencher at pH 2.6. Table 1 shows the Stern–Volmer constants K_{SV} to be higher (1.39) for the native state, intermediate (0.79) for the A-state, and the least (0.21) for the unfolded state, accompanied by a blue shift in λ_{max} . These results indicate that the tryptophan residues in the native state were more accessible to quenching by acrylamide than at low pH. The parameter f_a refers to the fraction of tryptophans accessible to the quencher and is obtained from the modified Stern–Volmer plots. It is the highest for pH 7.0, followed by pH 1.2, and the lowest at pH 2.6.

Size-exclusion chromatography and oligomeric status. Since CTA is a noncovalently associated dimer at pH 7.0, one possibility is that the intermediate seen in spectroscopically monitored denaturation is a monomeric form produced by dimer dissociation at low pH. To clarify this issue, size-exclusion chromatography was performed (Fig. 5a). The gel-filtration analysis of native CTA

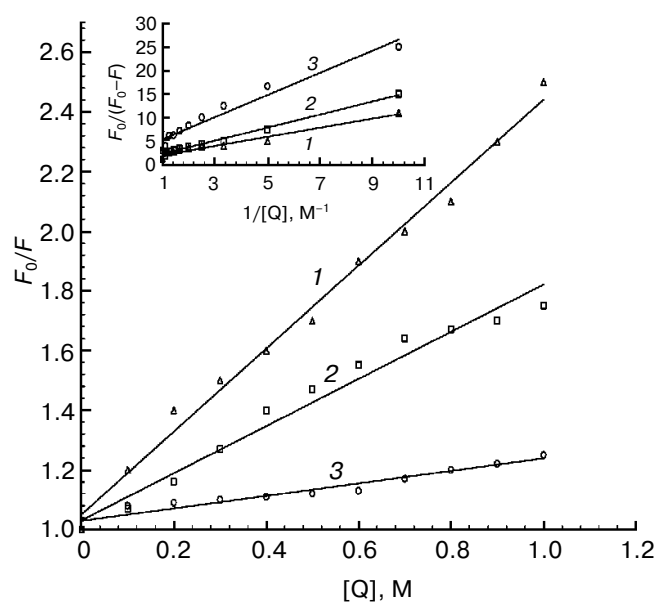


Fig. 4. Stern–Volmer plot and modified Stern–Volmer plot (inset) of acrylamide quenching. Native CTA at pH 7.0 (1), 2.6 (2), and 1.2 (3).

Table 1. Fluorescence parameters for acrylamide quenching of CTA

pH	K_{sv}	f_a , %	λ_{max} , nm
2.6	0.21	0.33	335
7.0	1.39	1.14	342
1.2	0.79	0.99	340

at pH 7.0 on Sephadex G-200 column confirms the dimeric nature of the protein (the elution volume corresponds to a molecular mass of 69 kDa). Gel filtration analysis at pH 2.6 and 1.2 showed increase in elution volume – the lectin peak appeared at a position of molecular mass of 34 kDa that corresponds to the monomer. It is interesting to note that completely unfolded monomer in 6 M GdnHCl was eluted in the void volume.

The pH has been known to have a marked effect on the structure of many globular proteins due to the ability of H^+ to influence electrostatic interactions. The interaction between two subunits of CTA is electrostatic. Polyacrylamide gel electrophoresis of CTA was performed under non-denaturing conditions to check the subunit status of the lectin in its three conformational states (Fig. 5b). CTA at pH 7.0 showed a single band and exists as the dimer (lane 3) with a smaller electrophoretic

mobility as compared to UA (lane 2). On decreasing the pH from 7.0 to 2.6, CTA becomes maximally positively charged, leading to oligomer dissociation and extended conformation. The A-state of CTA (lane 1) also showed a single prominent band, identically to the UA state, with high band intensity. Further decrease in pH to 1.4 adds more anions to solution, which interact with the positively charged centers on CTA, thus abolishing the electrostatic repulsive force and allowing the monomers to interact with each other. Thus, the A-state exists as a monomer, which tends to associate to form dimer. Concanavalin A has also shown pH-dependent dissociation and re-association of its subunits. The basic monomer subunit has a molecular mass of 25.5 kDa in solution at pH 2.0 and associates to form predominantly dimers at pH 5.0 and tetramers above pH 7.0.

Thermal denaturation. To check the structural properties of the above-obtained partially folded state, thermal denaturation studies were performed. Denaturation fraction (f_D) of lectin denatured at pH 7.0 and 1.2 as a function of temperature is shown in Fig. 6. The value of f_D of CTA at pH 7.0 was calculated assuming CTA at 30°C as the native state. The sigmoidal cooperative one-step transition between two states was observed for pH 7.0. The value of f_D of the A-state was calculated now assuming CTA at pH 1.2, 30°C, as native. The non-cooperative unfolding of CTA at pH 1.2 was indicative of its molten-globule like nature.

Functional property of CTA: carbohydrate binding. Figure 7 shows the effect of pH on the CTA–mucin pre-

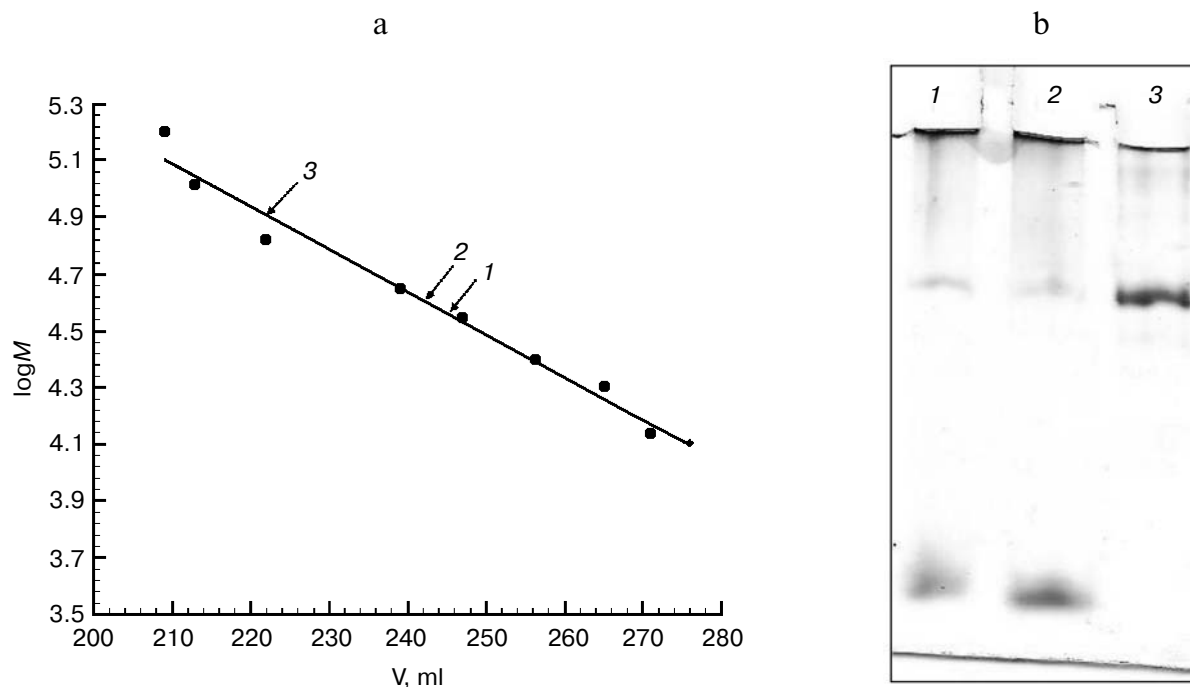


Fig. 5. Gel filtration of CTA on Sephadex G-200 column at pH 7.0 and 1.2 and PAGE. a) Native CTA migrated at the position of arrow 3 with the mass of 68.8 kDa. The A-state of CTA migrated at the position of arrow 2 (34.5 kDa). The UA state migrated at the position of arrow 1. b) Polyacrylamide gel (10%) electrophoregram of native CTA (lane 3), UA state (lane 2), and A-state (lane 1).

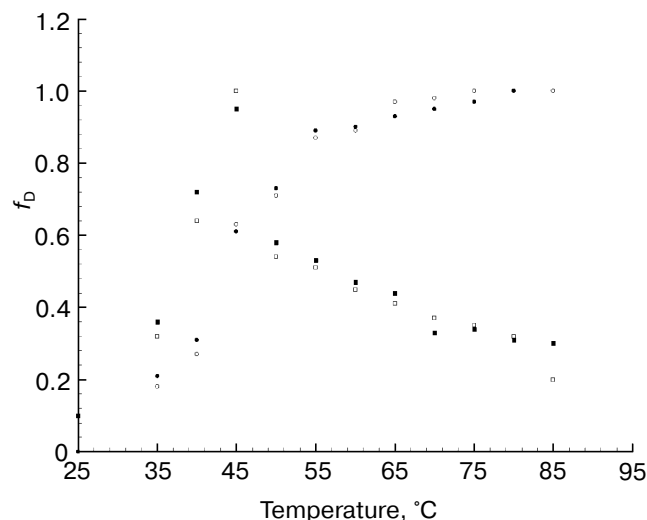


Fig. 6. Fraction of denatured protein (f_D) versus temperature as measured by change in MRE at 217 nm (○, □) and relative fluorescence intensity (●, ■) at pH 7.0 (○, ●) and 1.2 (□, ■). The protein concentration was 30 μ M for fluorescence and 15 μ M for far-UV CD (0.1 cm pathlength).

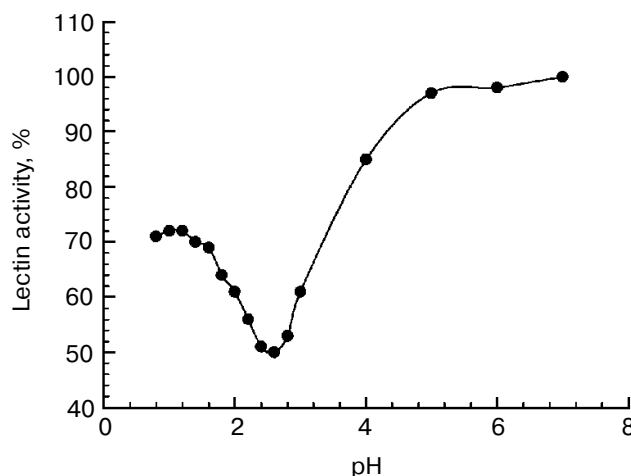


Fig. 7. The pH-dependence of *C. ternatea* agglutinin–mucin precipitation by turbidity measurements. Each tube contained 100 μ g lectin and 400 μ g mucin.

cipitin assay. When pH was decreased below 5.0, the activity also decreased. The decrease in activity was maximal at pH 2.6. Almost 50% of activity is lost, which is consistent with our far- and near-UV CD spectra, where 50 and 66% of the structure is lost, respectively. On further decreasing the pH, there was a regain in the activity, up to 72% at pH 1.2, indicating the rearranged secondary and tertiary structures.

DISCUSSION

Acids and bases are known to denature proteins by affecting their electrostatic interactions. Protonation of all ionizable side chains below pH 3.0 leads to charge–charge repulsion and consequently protein

unfolding. Further decrease in pH has no effect on the ionization state of the protein. On the other hand, the increase in anion concentration leads to refolding to an A-state.

Goto et al. [14] have proposed that acid denaturation of proteins leads to unfolding of the protein molecule due to intramolecular charge repulsion. However, proteins exhibit different behavior upon acid denaturation. Our studies on the acid-induced unfolding of the lectin reveal that CTA exhibits unfolding behavior characteristic of type I proteins, as classified by Fink et al. [30]. Acidic pH unfolding of CTA leads to the formation of a folded intermediate at pH 1.2 with “molten globule”-like characteristics. “Molten globules” are partially structured protein folding intermediates that adopt a native-like overall backbone topology in the absence of extensive tertiary

Table 2. Comparison of structural and functional propensities of intermediate states of CTA at different pH values

pH	Parameter						
	MRE at 217 nm	Relative fluorescence	Fluorescence emission maximum, nm	Relative ANS fluorescence	ANS fluorescence emission maximum, nm	Cooperativity (thermal denaturation)	Activity, %
7	−20.1	81	342	3	510	yes	100
2.6	−11	62	335	50	485	no	50
1.2	−14	80	340	119	480	no	72

interactions. It is important to determine the extent of specific tertiary structure present in molten globule and to understand the role of specific side-chain packing in stabilizing and specifying the molten globule structure. Wu and Kim [31] have identified a stabilizing hydrophobic core that corresponds to a previously identified structural domain and likely contains some native-like packing interactions. Moreover, the A-state of equine ferricytochrome *c* has native-like compactness, native-like helix content [32], a native helix–helix interaction, and one native heme ligand [33, 34]. Tertiary A-state interactions have been reported for α -lactalbumin [5, 30], RNase H [35], myoglobin [36], and ubiquitin [37].

Interestingly, the CTA intermediate, despite the partial loss of tertiary structure at pH 1.2, retains its carbohydrate binding activity to a considerable degree. The precipitation reaction involving CTA and mucin resembles an antigen–antibody reaction. Accordingly, CTA–ligand reaction leading to specific precipitation can be represented by the equilibria $\text{CTA} + \text{mucin} \leftrightarrow \text{complex (soluble)} \leftrightarrow \text{complex (precipitate)}$. It is the aggregation of the soluble complex, i.e. the second step that was monitored by the turbidity method in this study [12]. Solvent denaturation studies on concanavalin A and winged bean acidic agglutinin have shown that conformational stability of legume lectins reflects their different modes of quaternary association having functional property [38, 39]. The effect of low pH on CTA was studied using spectroscopic techniques (fluorescence, fluorescence quenching, ANS binding, and CD), size-exclusion chromatography, thermal denaturation, and carbohydrate binding specificity. A comparison is given in Table 2. Our results on the acid-induced molten globule-like intermediate of CTA at pH 1.2 shows evidence of an A-state with native-like tertiary as well as secondary structure. Results of spectroscopic studies on the reversibility of the A-state at pH 1.2 lead us to believe that the acid-induced unfolding of CTA is reversible. The structural similarity between the molten globule and native protein may have a significant bearing on understanding the protein folding problem. This state also retains carbohydrate binding property. The elucidation of the structure–function relationship of proteins using various biophysical tools will be important in understanding proteomics.

The authors are highly thankful for the facilities obtained at AMU Aligarh. We are also thankful to CSIR and UGC for financial support. A. N. is the recipient of a CSIR-SRF.

REFERENCES

1. Kuwajima, K. (1989) *Proteins*, **6**, 87–103.
2. Ptitsyn, O. B. (1995) *Trends Biochem. Sci.*, **20**, 376–379.
3. Goto, Y., and Fink, A. L. (1989) *Biochemistry*, **28**, 945–952.
4. Dryden, D., and Weir, M. P. (1991) *Biochim. Biophys. Acta*, **1078**, 94–100.
5. Song, J., Bai, P., Luo, L., and Peng, Z. Y. (2001) *Protein Sci.*, **10**, 53–62.
6. Colon, W., and Roder, H. (1996) *Nat. Struct. Biol.*, **3**, 1019–1025.
7. Barrick, D., Hughson, F. M., and Baldwin, R. L. (1994) *J. Mol. Biol.*, **237**, 588–601.
8. Jaenicke, R. (1991) *Biochemistry*, **30**, 3147–3161.
9. Naeem, A., Khan, A., and Khan, R. H. (2005) *Biochem. Biophys. Res. Commun.*, **331**, 1284–1294.
10. Ballery, N., Desmadril, M., Minard, P., and Yon, J. M. (1993) *Biochemistry*, **32**, 708–714.
11. Matousschek, A., Serrano, L., Meiering, E. M., Bycroft, M., and Ferscht, A. R. (1992) *J. Mol. Biol.*, **224**, 837–845.
12. Naeem, A., Khan, K. A., and Khan, R. H. (2004) *Arch. Biochem. Biophys.*, **432**, 79–87.
13. Goto, Y., and Nishikiori, S. (1991) *J. Mol. Biol.*, **222**, 679–686.
14. Goto, Y., Calciano, L. J., and Fink, A. L. (1990) *Proc. Natl. Acad. Sci. USA*, **87**, 573–577.
15. Kumar, D. P., Tiwari, A., and Bhatt, R. (2004) *J. Biol. Chem.*, **279**, 32093–32099.
16. Naeem, A., Haque, S., and Khan, R. H. (2007) *Protein J.*, **26**, 403–413.
17. Naeem, A., Ahmad, E., and Khan, R. H. (2007) *Int. J. Biol. Macromol.*, **41**, 481–486.
18. Davis, B. J. (1964) *Ann. N. Y. Acad. Sci.*, **121**, 404–407.
19. Lowry, D. H., Rosebrough, N. J., Farr, A. L., and Randall, R. J. (1951) *J. Biol. Chem.*, **193**, 265–275.
20. Stryer, L. (1965) *J. Mol. Biol.*, **13**, 482–495.
21. Stryer, L. (1968) *Science*, **162**, 526–540.
22. Semisotnov, G. V., Rodionova, N. A., Razgulyaev, O. I., Uversky, V. N., Gripas, A. F., and Gilmanshin, R. I. (1991) *Biopolymers*, **31**, 119–128.
23. Matulis, D., and Lovrien, R. (1998) *Biophys. J.*, **74**, 422–429.
24. Matulis, D., Baumann, C. G., Bloomfield, U. A., and Lovrien, R. E. (1999) *Biopolymers*, **49**, 451–458.
25. Muzammil, S., Kumar, Y., and Tayyab, S. (1999) *Eur. J. Biochem.*, **266**, 26–32.
26. Pawar, S. A., and Deshpande, V. V. (2000) *Eur. J. Biochem.*, **267**, 6331–6338.
27. Holzman, T. E., Dougherty, J. J., Brems, D. N., and Mackenzie, N. E. (1990) *Biochemistry*, **29**, 1255–1261.
28. Nandi, P. K. (1998) *Int. J. Biol. Macromol.*, **22**, 23–31.
29. Lala, A. K., and Kaul, P. (1992) *J. Biol. Chem.*, **267**, 19914–19918.
30. Fink, A. L., Calciano, C. T., Goto, Y., Kurotsu, T., and Palleros, D. R. (1994) *Biochemistry*, **33**, 12504–125011.
31. Wu, L. C., and Kim, P. S. (1998) *J. Mol. Biol.*, **280**, 175–182.
32. Goto, Y., Takahashi, N., and Fink, A. L. (1990) *Biochemistry*, **29**, 3480–3488.
33. Hamada, D., Kuroda, Y., Kataoka, M., Aimoto, S., Yoshimura, T., and Goto, Y. (1996) *J. Mol. Biol.*, **256**, 172–186.
34. Kataoka, M., Hagihara, Y., Mihara, K., and Goto, Y. (1993) *J. Mol. Biol.*, **229**, 591–596.
35. Raschke, T. M., and Marqusee, S. (1997) *Nat. Struct. Biol.*, **4**, 298–304.
36. Kay, M. S., and Baldwin, R. L. (1996) *Nat. Struct. Biol.*, **3**, 439–445.
37. Khorasanizadeh, S., Peters, I. D., and Roder, H. (1996) *Nat. Struct. Biol.*, **3**, 193–205.
38. Mitra, N., Srinivas, V. R., Ramya, T. N., Ahmad, N., Reddy, G. B., and Surolia, A. (2002) *Biochemistry*, **41**, 9256–9263.
39. Reddy, G. B., Srinivas, V. R., Ahmad, N., and Surolia, A. (1999) *J. Biol. Chem.*, **274**, 4500–4504.